Radiation properties of the accretion disk around a black hole in Einstein-Maxwell-scalar theory*

Mirzabek Alloqulov[1,2,3†]   Sanjar Shaymatov[4,5,2,6,7‡]   Bobomurat Ahmedov[2,8,9§]   Abdul Jawad[4,10♮]

[1]New Uzbekistan University, Movarounnahr street 1, Tashkent 100000, Uzbekistan
[2]Institute of Fundamental and Applied Research, National Research University TIIAME, Kori Niyoziy 39, Tashkent 100000, Uzbekistan
[3]University of Tashkent for Applied Sciences, Str. Gavhar 1, Tashkent 100149, Uzbekistan
[4]Institute for Theoretical Physics and Cosmology, Zhejiang University of Technology, Hangzhou 310023, China
[5]Central Asian University, Milliy Bog Street 264, Tashkent 111221, Uzbekistan
[6]National University of Uzbekistan, Tashkent 100174, Uzbekistan
[7]Power Engineering Faculty, Tashkent State Technical University, Tashkent 100095, Uzbekistan
[8]Ulugh Beg Astronomical Institute, Astronomy St 33, Tashkent 100052, Uzbekistan
[9]Institute of Theoretical Physics, National University of Uzbekistan, Tashkent 100174, Uzbekistan
[10]Department of Mathematics, COMSATS University Islamabad, Lahore Campus, Lahore-54000, Pakistan

Abstract: In this study, we explore the properties of a non-rotating black hole in the Einstein-Maxwell-scalar (EMS) theory and investigate the luminosity of the accretion disk surrounding it. We determine all the orbital parameters of particles in the accretion disk, including the radius of the innermost stable circular orbit (ISCO) with angular velocity, angular momentum, and energy. Further, we study the radiative efficiency for different values of black hole parameters. Finally, we analyze the flux, differential luminosity, and temperature of the accretion disk.

I. INTRODUCTION

Black holes are assumed to form as a result of the gravitational collapse of compact massive objects that have exhausted all their resources to resist gravity. Therefore, they are fascinating objects with a very attractive nature. The existence of black holes has been confirmed by recent gravitational wave [1, 2] and astronomical observations associated with the BlackHoleCam and EHT collaborations [3, 4]. These observational studies open up captivating avenues for forthcoming investigations to test remarkable aspects and gravitational properties of black holes in general relativity (GR) and modified theories of gravity.

It is a fact that astrophysical black holes can have three parameters in most cases, including black hole mass M, spin a, and charge Q. According to recent astronomical observations, black holes can be considered as rotating [5−10] as well as charged black holes that correspond to the Reissner-Nordström (RN) black hole solution characterized by M and Q. This well-known RN solution in GR

was first proposed by H. Reissner in 1916 [11]. It was also independently considered by G. Nordström in 1918 [12] with linear Maxwell electrodynamics. Afterwards, the remarkable aspects of the RN black hole were discussed by addressing the motion of neutral and charged particles [13, 14]. Several astrophysical mechanisms have since been proposed in relation to how black holes can possess electric charge. For example, the balance between gravitational and Coulomb forces for charged particles allows black holes to have a positive net electric charge at the compact object's near surface [15, 16], and the irradiating photons also give rise to charged matter at the surface [17]. Another way is that the twisted magnetic field lines due to the black hole spin can produce the induced charge, referring to the well-known Wald mechanism [18]. Later, an exact rotating Schwinger dyon solution was proposed as a charged black hole solution with mass M, electric charge Q_e, magnetic charge Q_m, and spin a [19, 20]. Charged black hole solutions that are free of the physical singularity $r = 0$ also exist, which are referred to as regular black hole solutions coupled to non-linear elec-

trodynamics (NED) in GR [21−37] addressing various situations. As these solutions can avoid physical singularity, they have since been studied and tested for various possible cases [38−40].

Einstein gravity is known as a best theory in the strong field regime. The GR can also be extended to the low energy limit of the string theory associated with the dilaton scalar field as an extra term added to the action that refers to the Einstein-Hilbert action, including the axion, gauge, and dilaton fields [41, 42]. In this context, the authors of Ref. [43] considered the heterotic string theory including the scalar dilaton field that is coupled to the electromagnetic field tensor. On these lines, there has been an extensive analysis [42−47] addressing the causal structures and thermodynamic properties of black hole solutions associated with the dilaton field. Several investigations have also been conducted on black hole solutions in various extended theories [48−52]. In the context of extended theories of gravity, some approaches including quantum features have been proposed and analyzed so as to give a peculiarity to the literature (see, for example, in [53−60]).

From the theoretical and observational studies, the existence of an accretion disk around black holes is expected to be the primary source of information about gravity and geometry in the strong field regime. It can also enable very potent tests for probing unknown aspects of high energy phenomena occurring in the close vicinity of black holes [61]. Therefore, it has value to consider important and valuable insights of the spacetime geometry in the strong field regime that can have a significant impact on the test particle geodesics and can result in changing observable quantities, that is, the innermost stable circular orbit (ISCO) and accretion disk parameters. With this in view, having confidence with the conclusions from observations related to the accretion disks is significantly important. Thus, observational data on the thin accretion disk though the anticipated thermal spectra could play a decisive role in testing the gravity in the strong field regime. With this motivation in mind, in this work, we explore the properties of an interesting solution describing a non-rotating black hole in the Einstein-Maxwell-scalar (EMS) theory. We investigate remarkable aspects and radiation properties of the accretion disk around a black hole on the basis of the geometrically thin Novikov–Thorne model as an optically thick disk. We also analyze the ISCOs around black holes in the EMS theory. Further, we represent the radiation properties of the accretion disk, that is, the temperature and spectral energy distributions for a thin Novikov–Thorne disk as a consequence of the comparison with the results of the standard Schwarzschild case in the context of GR.

The paper is organized as follows. We briefly review the solution of the charged black hole in the EMS theory in Sec. II. Sec. III is devoted to the study of charged test particle dynamics around the black hole and the geometrically thin Novikov-Thorne model for the accretion disk. We discuss the flux of the radiant energy over the accretion disk, accretions disk's radiative efficiency, temperature profile, and differential luminosity in Sec. IV. We summarize our results in Sec. V. Throughout this paper, we use the $(−, +, +, +)$ signature for the spacetime metric and system of units in which we set $G = c = 1$.

II. STATIC BLACK HOLES IN EINSTEIN-MAXWELL-SCALAR THEORY

Here, we review the charged black hole solutions in EMS theory. To this end, we first write the action as follows [42, 62]:

$$S = \int \mathrm{d}^4 x \sqrt{-g} \left[R - 2\nabla_\alpha \phi \nabla^\alpha \phi - K(\phi) F_{\alpha\beta} F^{\alpha\beta} - V(\phi) \right],$$

with the covariant derivative ∇_α, Ricci scalar R, and massless scalar field ϕ. $F_{\alpha\beta}$ and $K(\phi)$ refer to the electromagnetic field tensor and the function of scalar field, respectively, that describes the coupling function between the electromagnetic and dilaton fields. $V(\phi)$ refers to the scalar potential associated with the cosmological constant Λ in the frame of the EMS theory and describes the black hole in the de-Sitter universe coupled with the dilaton field, that is, $V(\phi) = \Lambda \left(e^{2\phi} + 4 + e^{-2\phi} \right) /3$ [63]. However, we further restrict ourselves to the black hole solution with vanishing cosmological constant, that is, $V(\phi) = 0$. With this in view, the metric describing a static and spherically symmetric black hole solution in the Schwarzschild coordinate system is then given by [62]

$$\mathrm{d}s^2 = -U(r)\mathrm{d}t^2 + \frac{\mathrm{d}r^2}{U(r)} + f(r) \left(\mathrm{d}\theta^2 + \sin^2\theta \mathrm{d}\varphi^2 \right), \quad (1)$$

where $U(r)$ and $f(r)$ refer to radial functions given in terms of the function $K(\phi)$ that is written as

$$K(\phi) = \frac{2e^{2\phi}}{\beta e^{4\phi} + \beta - 2\gamma}. \quad (2)$$

Hence, these two functions are written in the following forms:

$$f(r) = r^2 \left(1 + \frac{\gamma Q^2}{Mr} \right),$$
$$U(r) = 1 - \frac{2M}{r} + \frac{\beta Q^2}{f(r)}, \quad (3)$$

with mass M and electric charge Q of the black hole. We note that the new terms are given with β and γ, which are dimensionless constants of the static black hole solution

in EMS theory. The metric functions $f(r)$ and $U(r)$ reduce to the Schwarzschild case in the limit of $\beta = 0$ and $\gamma = 0$, and to the Reissner-Nordström case in the limit of $\gamma = 0$ and $\beta = 1$. However, it is worth noting that the functions $f(r)$ and $U(r)$ present the dilation solution in the limit of $\beta = 0$ and $\gamma = -1$ (i.e., $K(\phi) = e^{2\phi}$ and $V(\phi) = 0$ [42, 43]).

We assume that the vector and the dilaton fields depend on the radial coordinate only as shown in Ref. [62], and thus, their radial form can be defined by

$$A_t(r) = \frac{Q}{r}\left[\gamma - \frac{\beta}{2}\left(1 + \frac{r^2}{f(r)}\right)\right], \tag{4}$$

$$\phi(r) = -\frac{1}{2}\ln\left(\frac{f(r)}{r^2}\right). \tag{5}$$

Further, the condition $U(r) = 0$ with respect to r solves to give the black hole horizon as

$$\frac{r_h}{M} = 1 - \frac{\gamma Q^2}{2M^2} + \sqrt{1 + \frac{Q^2(\gamma - \beta)}{M^2} + \frac{\gamma^2 Q^4}{4M^4}}. \tag{6}$$

In Fig. 1, we demonstrate the radial profiles of the radial function $U(r)$ for various combinations of the EMS parameters β and γ and also for the black hole charge. As can be observed from Fig. 1, the zeros of the metric function imply the location of black hole horizons. Fig. 1 shows that Cauchy and event horizons become close to each other for large values of β. In addition, the black hole event horizon increases for negative values of γ, whereas it decreases for $\gamma > 0$.

Let us now examine the characteristics of the extremes in the black hole charge and the minimum in the event horizon radius by setting the following condition:

$$U(r) = U'(r) = 0. \tag{7}$$

The above condition allows one to obtain the radius and charge expressions as follows:

$$\frac{(r_h)_{\min}}{M} = 2 - \frac{\beta}{\gamma} + \frac{\sqrt{\beta^2 - 2\beta\gamma}}{\gamma}, \tag{8}$$

$$\frac{Q^2_{\text{extr}}}{M^2} = \frac{2\left(\beta - \sqrt{\beta^2 - 2\beta\gamma} - \gamma\right)}{\gamma^2}. \tag{9}$$

In Fig. 2 we show the dependence of the minimum values of the outer horizon and extreme values of the black hole charge from the parameter γ for the different values of β. The solid lines stand for the minimum event horizon, whereas the dashed ones stand for the extreme charge. As can be observed from Fig. 2, the minimum radius of the outer horizon decreases with an increase in the value of γ, and it also decreases with an increase in the value of β at $\gamma < 0$. Similarly, the extreme in Q also decreases at $\gamma < 0$. The event horizon becomes zero in the case in which β reaches its critical value, thus implying that β must be less than β_{cr}. The critical value of β increases with the increase in parameter γ.

Our numerical analysis shows that for all possible values of parameter γ, the following conditions are always satisfied:

$$\lim_{\beta \to 0}\{(r_h)_{\min}, Q_{\text{extr}}\} = \{2M, 0\},$$

and

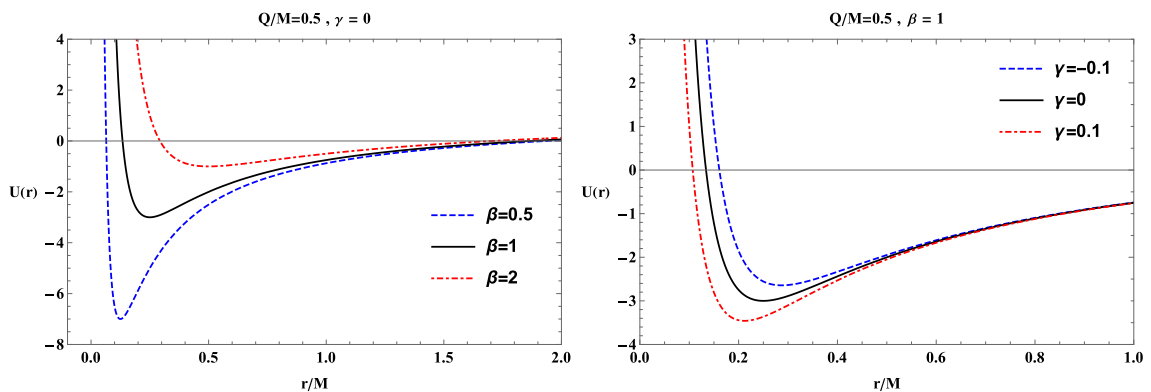$$\lim_{\beta \to \beta_{\max}}\{(r_h)_{\min}, Q_{\text{extr}}\} = \{0, Q_{\text{extr}}\}.$$

Fig. 1. (color online) Radial dependence of the metric function $U(r)$ plotted for the different values of parameters β and γ in the left and right panels, respectively.
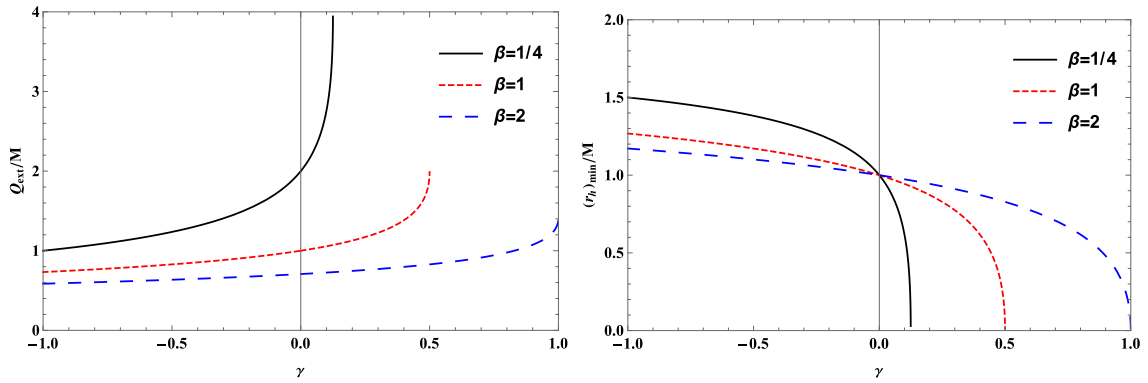
Fig. 2. (color online) Critical values of black hole charge (left panel) and minimal radius of the horizon (right panel) as functions of the parameter γ for various combinations of β.

The upper value of $\beta_{\max}$ (Q_{extr}) increases (decreases) as parameter γ increases. Together with Eqs. (8) and (9), one can easily find the following relations:

$$\beta_{\max} = 2\gamma, \qquad \frac{Q_{\mathrm{extr}}}{M} = \sqrt{\frac{2}{\gamma}} . \qquad (10)$$

In Table 1, we present the critical values of β and corresponding values of Q_{extr} for the given values of γ.

III. NOVIKOV-THORNE MODEL OF THE ACCRETION DISK

Following the Novikov-Thorne model [64], one can let the accretion disk be optically thick and geometrically thin in the close vicinity of the EMS black hole. However, the accretion disk is really very thin in vertical size because it is extended to the horizontal size. This in turn gives rise to a negligible size in terms of the vertical size in comparison with its long horizontal extension. Therefore, its height h is much smaller than the radius of the disk r extended in the horizontal direction, that is, $h \ll r$. From this property of the thin accretion disk formed in the surrounding environment of the EMS black hole and from the hydrodynamic equilibrium of the thin disk, the vertical entropy and pressure gradients are regarded as negligible in the accreting matter. The heat generated due to the stress and dynamical friction cannot be accumulated in the accretion disk that is efficiently cooled as stated by the thermal radiation on the disk surface. Hence, this leads to the stabilized thin disk, whose inner edge is then located at a stable orbit around the black hole, thus taking the Keplerian motion for the plasma accreting in stable orbits.

We now define the bolometric luminosity of the accretion disk that is given by [65, 66]

$$\mathcal{L}_{bol} = \eta \dot{M} c^2 , \qquad (11)$$

Table 1. Extremes of black hole charge and critical value of γ for different values of β when the event horizon is zero.

γ	$\beta_{\max}$	Q_{extr}/M
1/8	1/4	4
1/4	1/2	$2\sqrt{2}$
3/8	3/4	4/3
1/2	1	2
3/4	3/2	$2\sqrt{2}/3$
1	2	$\sqrt{2}$

where $\dot{M}$ and η refer to the rate of accretion matter that falls into the black hole and the energy efficiency of the accretion disk, respectively. It is known from an astrophysical point of view that some issues exist in observing the bolometric luminosity, depending on the black hole parameters and its type. It does, therefore, become very important to measure the bolometric luminosity through the theoretical analysis and models. To this end, it is valuable to define the energy efficiency of the accretion disk around black holes, which is the highest energy that can be mined out via the the accretion disk, as that of matter falling into the black hole. Hence, the energy efficiency is increasingly important to explain the nature of the accretion process due to the fact that the rest mass-accreting matter turns into the electromagnetic radiation that goes out from the central object. One can then further determine the energy efficiency that stems from the radiation rate of the photon energy that is emitted from the disk surface [67, 68]. Thus, the efficiency can be determined via the measured energy at the ISCO [69] in the case when the photons emitted from the disk escape to infinity, that is [70]:

$$\eta = 1 - \mathcal{E}_{\mathrm{ISCO}} . \qquad (12)$$

The above expression for the measured energy at the ISCO allows one to find the radiative efficiency η for the

emitted photon from the disk. Therefore, it is essential to determine the ISCO parameters, that is, r_{ISCO}, $\mathcal{E}_{\text{ISCO}}$, and $\mathcal{L}_{\text{ISCO}}$. For that purpose, one needs to consider the test particle dynamics around electrically charged EMS black holes. It is well-known that the standard form of the effective potential for the radial motion of the test particle can generally be defined by [71]

$$V_{\text{eff}}(r) = -1 + \frac{\mathcal{E}^2 g_{\phi\phi} + 2\mathcal{E}\mathcal{L}g_{t\phi} + \mathcal{L}^2 g_{tt}}{g_{t\phi}^2 - g_{tt}g_{\phi\phi}}, \qquad (13)$$

with the specific energy $\mathcal{E} = E/m$ and angular momentum $\mathcal{L} = L/m$. Here, we note that the metric functions are given by $g_{tt} = U(r)$ and $g_{\phi\phi} = f(r)\sin^2\theta$ with $g_{t\phi} = 0$ for a static and spherically symmetric black hole. These two conserved quantities can be written in terms of metric tensors as follows:

$$\mathcal{E} = -\frac{g_{tt}}{\sqrt{-g_{tt} - \Omega^2 g_{\phi\phi}}}, \qquad (14)$$

and

$$\mathcal{L} = \frac{\Omega g_{\phi\phi}}{\sqrt{-g_{tt} - \Omega^2 g_{\phi\phi}}}. \qquad (15)$$

Similarly, the orbital angular velocity of the test particle is also given by [72−74]

$$\Omega = \frac{\mathrm{d}\phi}{\mathrm{d}t} = \sqrt{-\frac{g_{tt,r}}{g_{\phi\phi,r}}}. \qquad (16)$$

Here, we note that we further restrict motion to the equatorial plane, that is, $\theta = \pi/2$. According to the model, the accretion disk's inner edge around the black hole can be determined by the ISCO radius that is defined by the following set of conditions for the effective potential:

$$V_{\text{eff}}(r) = 0, \quad V'_{\text{eff}}(r) = 0, \quad V''_{\text{eff}}(r) = 0. \qquad (17)$$

Let us then turn to the charged particle dynamics around EMS black holes. To that end, we can now define the effective potential for the charged particles moving

around the EMS black hole [75],

$$V_{\text{eff}}^{\pm}(r) = qA_t \pm \sqrt{U(r)\left(1 + \frac{\mathcal{L}^2}{f(r)\sin^2\theta}\right)}. \qquad (18)$$

The above effective potential has two parts, the column and gravitational interaction parts. Two different solutions exist because the effective potential can behave as symmetry in the following replacements $qQ \to -qQ$: $V_{\text{eff}}^+ \to -V_{\text{eff}}^-$ and $V_{\text{eff}}^- \to -V_{\text{eff}}^+$. However, we will restrict ourselves to the effective potential V_{eff}^+ that corresponds to the positive energy for physically meaningful timelike motion and for analysing the charged particle's dynamics. Taking V_{eff}^+ into consideration, we can further find the ISCO values of the charged particle, that is, r_{ISCO}, $\mathcal{E}_{\text{ISCO}}$, and $\mathcal{L}_{\text{ISCO}}$. It is worth noting that we decided to explore the ISCO values numerically. The results are presented in Table 2. As can be observed from the results on the ISCO radius determining the inner edge of the accretion disk, it decreases as a consequence of an increase in the value of the dimensionless parameter β, whereas it increases under the effect of parameter γ. Taking all together, we then analyse the energy efficiency of the accretion disk around the black hole in EMS theory. The value of the energy efficiency is presented in Table 2. As can be observed from the results, the radiative efficiency increases with an increase in the value of parameter β, whereas it decreases as a consequence of the impact of parameter γ. Note that the Schwarzschild black hole case can be obtained in the limit of $\beta = 0$ and $\gamma = 0$. At this point, the efficiency is equal to $\eta \approx 5.7\%$ [76]. Similarly, the following limit, $\beta = 1$ and $\gamma = 0$, refers to the RN black hole case. The radiative efficiency is then evaluated to be $\eta \approx 7.5\%$ in the RN black hole case.

IV. RADIATIVE PROPERTIES OF THE ACCRETION DISK AROUND A CENTRAL COMPACT OBJECT

In this section, we study the flux produced by an accretion disk of the EMS black hole. We note that an accretion disk consists of gas and dust moving on stable orbits of a black hole or neutron star. The gas and dust can

Table 2. Value of the innermost stable circular orbit (ISCO) radius and radiative efficiency of the accretion disk tabulated for the different values of parameter β in the possible cases of parameter γ. Note that we have set $q = 0.5$ and $Q = 0.5$.

| β | $\gamma = -1$ | | $\gamma = 0$ | | $\gamma = 1$ | |
	r_{ISCO}	$\eta(\%)$	r_{ISCO}	$\eta(\%)$	r_{ISCO}	$\eta(\%)$
0.0	5.76641	7.50318	6.0	5.7191	6.2865	4.0603
0.5	5.61325	8.41598	5.82216	6.58717	6.05386	4.89047
1.0	5.46477	9.35293	5.65896	7.47554	5.85509	5.74132
2.0	5.16738	11.3155	5.35546	9.31973	5.51641	7.50318

lose their energy and angular momentum owing to the background geometry when they start moving around the compact object. As a result, the orbits of gas and dust move to the inner edge of the accretion disc so that they fall towards the compact object. This process ends up with accretion disk radiation, in which the gas and dust can heat up and emit radiation. We further expect that the accretion disk radiation can be affected by the EMS black hole parameters. In particular, the black hole charge can affect the gas and dust in the accretion disk around the black hole, thus resulting in highly ionized gas and dust in the accretion disk around the black hole. As a consequence of the ionization process, the high energy radiation can be emitted in the form of X-rays that can be detected. The radiation of the accretion disk around a black hole in the EMS theory is expected to be a potent test to explain valuable and remarkable aspects of the accretion disk and can also lead to serious implications from the observational point of view. The flux of the electromagnetic radiation can be defined by the following equation [67, 77, 78]:

$$\mathcal{F}(r) = -\frac{\dot{M}_0}{4\pi \sqrt{g}} \frac{\Omega_{,r}}{(E-\Omega L)^2} \int_{r_{\rm ISCO}}^{r} (E-\Omega L)L_{,r}{\rm d}r, \qquad (19)$$

with the determinant of the three-dimensional subspace $g = \sqrt{-g_{tt}g_{rr}g_{\phi\phi}}$ with (t,r,ϕ) coordinates. In the above equation, the quantity $\mathcal{F}(r)$ can be defined as the function of $\dot{M}_0$ that can be regarded as unknown and corresponds to the accretion rate of the disk mass. However, we can set $\dot{M}_0 = 1$ for further analysis.

Using Eqs. (14) and (15) we further derive the flux of the electromagnetic radiation. It does however turn out that it is complicated to derive the analytical expression of the flux, and thus, we resort to it numerically, as shown in Fig. 3. As can be observed from Fig. 3, the shape of the flux of the electromagnetic radiation increases/decreases under the effect of the γ parameter as compared with the RN case, depending on its sign. However, it increases as a consequence of an increase in the value of black hole charge Q and parameter β. In the top-left panel of Fig. 3, we show the flux of the electromagnetic radiation for the Schwarzschild and RN black hole cases. From Fig. 3, it can be easily observed that the black hole charge increases the value of the flux of the electromagnetic radiation. In addition, the flux of the black body radiation can be written as $\mathcal{F}(r) = \sigma T^4$ with σ as the Stefan-Boltzmann constant. The radial dependence of the disk temperature and energy is further shown in Fig. 4 for various values of black hole charge. In this
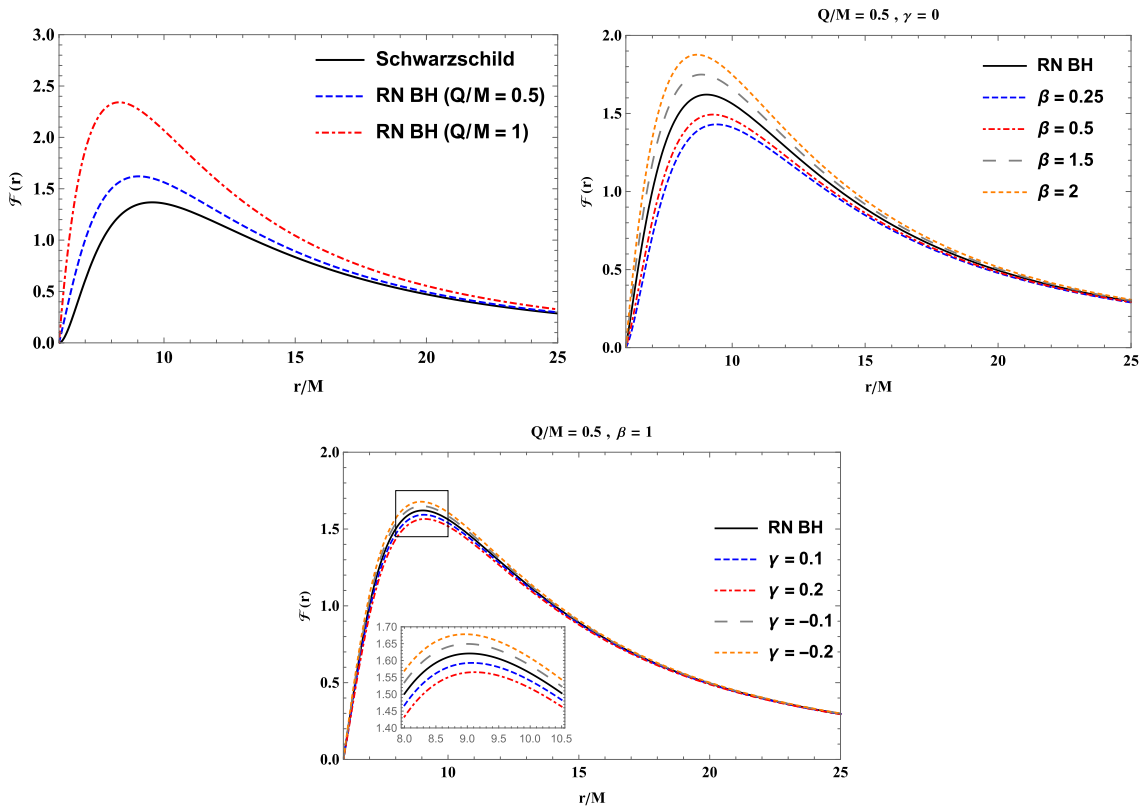

Fig. 3.　(color online) Radial dependence of the flux of electromagnetic radiation of the accretion disk on different values of Q, β, and γ, plotted for the black hole in EMS theory. Numerical evaluation of the flux $\mathcal{F}$ divided by 10^{-5} of the accretion disk as a function of r/M.
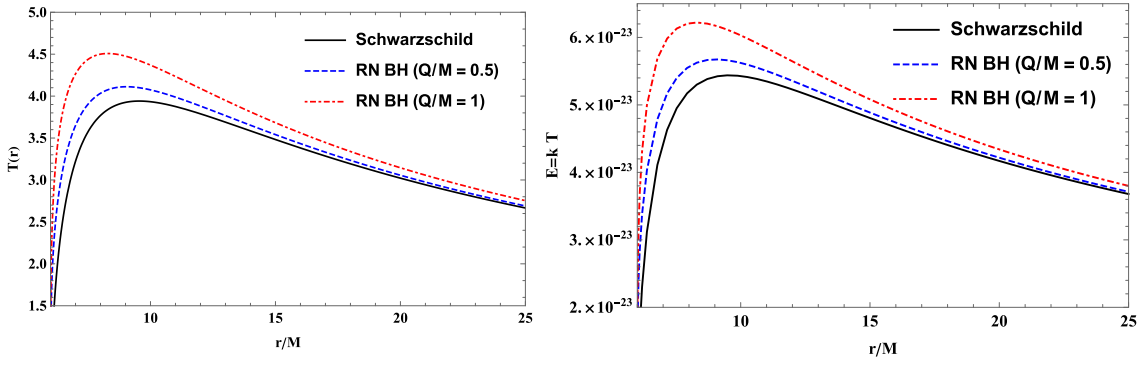
Fig. 4.   (color online) Radial dependence of the temperature and energy of the accretion disk plotted in the left and right panels, respectively, for different values of black hole charge Q in the case of fixed $\gamma = 0$ and $\beta = 1$.

graph, we select $\beta = 0$ & $\gamma = 0$ and $\beta = 1$ & $\gamma = 0$ for the Schwarzschild and Reissner-Nordström black holes, respectively. As can be observed from Fig. 4, the temperature and energy of the accretion disk around the EMS black hole increase with increasing black hole charge Q.

To be more informative, we plot the temperature through the "color map" in Fig. 5. From Fig. 5, it can be clearly observed that the dark region lies inside the accretion disk's inner edge, whereas the red parts refer to the regions where the temperature of the disk can reach its maximum value.

We then turn to another important quantity referred to as the differential luminosity. It can be expressed as follows [67, 77, 78]:

$$\frac{\mathrm{d}\mathcal{L}_\infty}{\mathrm{d}\ln r} = 4\pi r \sqrt{g} E \mathcal{F}(r). \tag{20}$$

We assume that the radiation emission can be described by black body radiation. Keeping this in mind, one can

then define the spectral luminosity $\mathcal{L}_{\nu,\infty}$ as a function of the radiation frequency ν at infinity [69, 79, 80] as follows:

$$\nu \mathcal{L}_{\nu,\infty} = \frac{60}{\pi^3} \int_{r_{\mathrm{ISCO}}}^{\infty} \frac{\sqrt{g} E}{M_T^2} \frac{(u^t y)^4}{\exp\left[\frac{u^t y}{(M_T^2 \mathcal{F})^{1/4}}\right] - 1}, \tag{21}$$

with $y = h\nu/kT_\star$, where h and k respectively refer to the Planck constant and constant of Boltzmann, as well as the total mass M_T. In addition, $T_\star$ corresponds to the characteristic temperature and has a relation with the Stefan-Boltzmann law, that is, $\sigma T_\star = \frac{\dot{M}_0}{4\pi M_T^2}$, where σ accordingly refers to the Stefan-Boltzmann constant. Another important quantity is the differential luminosity. The radial dependence of the differential luminosity is represented in Fig. 6. The electromagnetic radiation flux of the accretion disk can be scaled in powers of 10^{-5}. The differential luminosity of the accretion disk depends on the flux
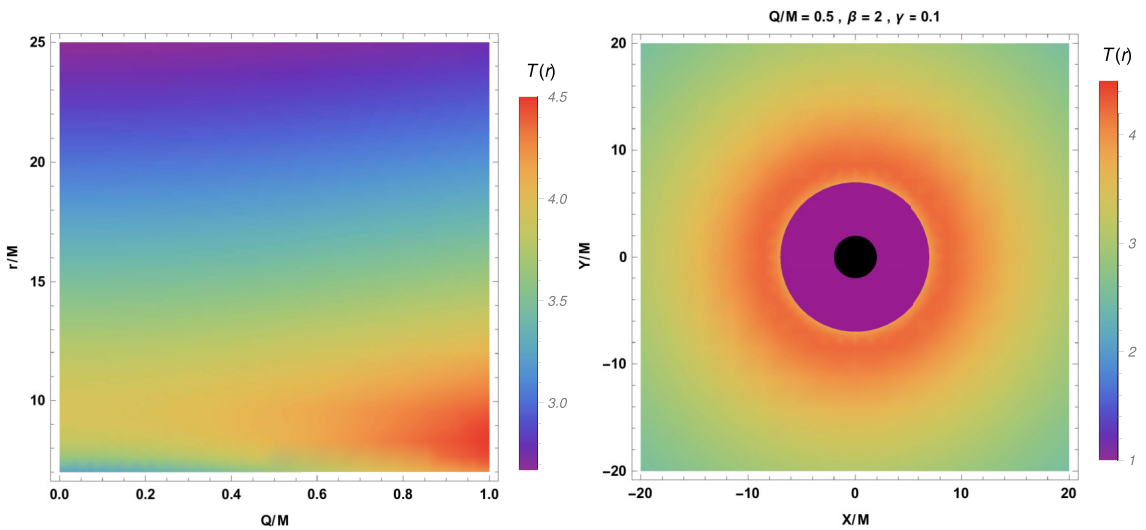

Fig. 5.   (color online) Left panel: temperature profile of the radial dependence of black hole charge. Right panel: temperature profile on the equatorial $X - Y$ plane in the form of density plot. Here, the Cartesian coordinates are defined by X and Y.
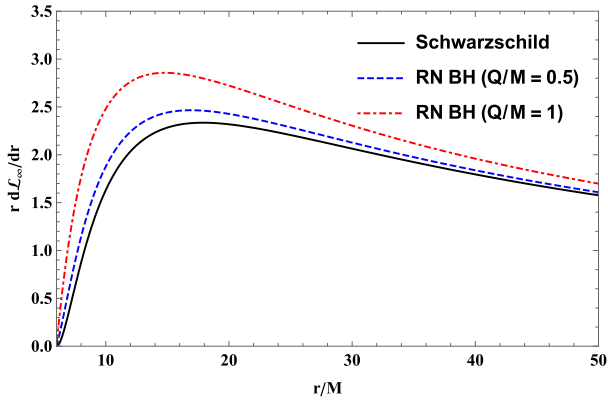
Fig. 6. (color online) Radial dependence of the differential luminosity of the accretion disk scaled in powers of 10^{-2} plotted as a result of the numerical evaluation.

by the relation given in Eq. (20). Therefore the value of the differential luminosity can be of the order of 10^{-2}. As can be observed, the value of the differential luminosity increases as a consequence of an increase in the value of black hole charge Q.

V. CONCLUSIONS

In this paper, we studied the radiation properties of the accretion disk around black holes in EMS theory as the accretion disk radiation can be affected by the EMS black hole parameters. The theoretical study of the accretion disk radiation around a black hole in EMS theory is expected to be a potent test to explain its valuable properties and the astrophysical observations. We can summarize the main results of our research as follows:

● We extensively studied the behavior of metric func-

tions in Fig. 1 and we found the horizon behaviour of the black hole in EMS theory. In addition, we obtained the extreme values of the black hole parameters using the equation for the horizon. We present the results for the extreme value of black hole parameters in Table 1.

● We also investigated the effective potential for the charged particles. On the basis of the effective potential, we further found the ISCO radius numerically and present the results in Table 2. We found that parameters γ and β have significant influence on the the ISCO radius of the charged particles.

● Further, we explored the radiative efficiency and present the results in Table 2. It was shown that the radiative efficiency increases with increasing parameter β, while it decreases as a consequence of an increase in the value of parameter γ.

● Finally, we considered the radiative properties of the black hole accretion disk, that is, we explored the flux, temperature, and spectral and differential luminosities of the black hole accretion disk. We show the results in Figs. 3−6. It was found that the black hole electric charge increases the flux of the electromagnetic radiation in EMS theory. Similarly, the temperature and energy of the accretion disk increase due to the impact of the black hole charge, as can be observed in the graph of temperature in the form of a density-plot in Fig. 5.

ACKNOWLEDGMENTS

References

[1] B. P. Abbott and *et al*. (Virgo and LIGO Scientific Collaborations), Phys. Rev. Lett. **116**, 061102 (2016), arXiv:1602.03837[gr-qc]

[2] B. P. Abbott and *et al*. (Virgo and LIGO Scientific Collaborations), Phys. Rev. Lett. **116**, 241102 (2016), arXiv:1602.03840[gr-qc]

[3] K. Akiyama and *et al*. (Event Horizon Telescope Collaboration), Astrophys. J. **875**, L1 (2019), arXiv:1906.11238[astro-ph.GA]

[4] K. Akiyama and *et al*. (Event Horizon Telescope Collaboration), Astrophys. J. **875**, L6 (2019), arXiv:1906.11243[astro-ph.GA]

[5] C. Bambi, Rev. Mod. Phys. **89**, 025001 (2017), arXiv:1509.03884[gr-qc]

[6] D. J. Walton, E. Nardini, A. C. Fabian *et al*., Mon. Not. R. Astron. Soc. **428**, 2901 (2013), arXiv:1210.4593[astro-ph.HE]

[7] A. R. Patrick, J. N. Reeves, D. Porquet *et al*., Mon. Not. R.

Astron. Soc. **411**, 2353 (2011), arXiv:1010.2080[astro-ph.HE]

[8] A. R. Patrick, J. N. Reeves, A. P. Lobban *et al*., Mon. Not. R. Astron. Soc. **416**, 2725 (2011), arXiv:1106.2135[astro-ph.HE]

[9] Y. Tan, J. X. Wang, X. W. Shu *et al*., Astrophys. J. **747**, L11 (2012), arXiv:1202.0400[astro-ph.HE]

[10] L. C. Gallo, G. Miniutti, J. M. Miller *et al*., Mon. Not. R. Astron. Soc. **411**, 607 (2011), arXiv:1009.2987[astro-ph.HE]

[11] H. Reissner, Annalen der Physik **355**, 106 (1916)

[12] G. Nordström, Koninklijke Nederlandse Akademie van Wetenschappen Proceedings Series B Physical Sciences **20**, 1238 (1918)

[13] D. Pugliese, H. Quevedo, and R. Ruffini, Phys. Rev. D **83**, 104052 (2011), arXiv:1103.1807[gr-qc]

[14] D. Pugliese, H. Quevedo, and R. Ruffini, Phys. Rev. D **83**, 024021 (2011), arXiv:1012.5411[astro-ph.HE]

[15] M. Zajacek and A. Tursunov, The Observatory **139**, 231 (2019), arXiv:1904.04654[astro-ph.GA]

[16] J. Bally and E. R. Harrison, Astrophys. J. **220**, 743 (1978)
[17] J. C. Weingartner, B. T. Draine, and D. K. Barr, Astrophys. J. **645**, 1188 (2006), arXiv:astro-ph/0601296[astroph]
[18] R. M. Wald, Phys. Rev. D **10**, 1680 (1974)
[19] M. Kasuya, Phys. Rev. D **25**, 995 (1982)
[20] S. Shaymatov, P. Sheoran, R. Becerril *et al.*, Phys. Rev. D **106**, 024039 (2022)
[21] J. M. Bardeen, in Proc. Int. Conf. GR5, Tbilisi, Vol. 174 (sn, 1968) p. 174
[22] E. Ayón-Beato and A. Garcıa, Phys. Rev. Lett. **80**, 5056 (1998)
[23] E. Ayon-Beato and A. Garcia, General Relativity and Gravitation **31**, 629 (1999)
[24] K. A. Bronnikov, Phys. Rev. D **63**, 044005 (2001)
[25] C. Bambi and L. Modesto, Physics Letters B **721**, 329 (2013)
[26] Z.-Y. Fan and X. Wang, Phys. Rev. D **94**, 124027 (2016)
[27] L. Balart, G. Panotopoulos, and Á. Rincón, Fortschritte der Physik **71**, 2300075(2023)
[28] A. Rincon and G. Gómez, *Quasinormal modes and shadow in einstein maxwell power-yang-mills black hole*, (2023), arXiv: 2308.11756[gr-qc]
[29] L. Balart, S. Belmar-Herrera, G. Panotopoulos *et al.*, Annals of Physics **454**, 169329 (2023)
[30] S. I. Kruglov, Gravit. Cosmol. **29**, 57 (2023)
[31] S. I. Kruglov, Universe **9**, 24 (2022)
[32] S. Kruglov, Phys. Lett. B **822**, 136633 (2021)
[33] G. Panotopoulos, Axioms **9**, 33 (2020)
[34] Ángel Rincón, E. Contreras, P. Bargueño *et al.*, Phys. Dark Universe **31**, 100783 (2021)
[35] G. Panotopoulos and Ángel Rincón, *Quasinormal modes of regular black holes with non linearelectrodynamical sources*, (2019), arXiv: 1904.10847[grqc]
[36] Á. Rincón and G. Panotopoulos, Phys. Rev. D **97** (2018)
[37] G. Panotopoulos and Á. Rincón, Int. J. Mod. Phys. D **27**, 1850034 (2018)
[38] Z. Stuchlík and J. Schee, Int. J. Mod. Phys. D **24**, 1550020 (2015)
[39] J. Schee and Z. Stuchlík, Journal of Cosmology and Astroparticle Physics **2015**, 048 (2015)
[40] C. Bambi and D. Malafarina, Phys. Rev. D **88**, 064022 (2013)
[41] M. B. Green, J. H. Schwarz, and E. Witten, *Superstring theory. Volume 1 - Introduction* (1987).
[42] G. Gibbons and K. ichi Maeda, Nucl. Phys. B **298**, 741 (1988)
[43] D. Garfinkle, G. T. Horowitz, and A. Strominger, Phys. Rev. D **43**, 3140 (1991)
[44] T. Koikawa and M. Yoshimura, Phys. Lett. B **189**, 29 (1987)
[45] Dieter Brill, Gary T. Horowitz, Phys. Lett. B **262**, 437 (1991)
[46] B. Harms and Y. Leblanc, Phys. Rev. D **46**, 2334 (1992)
[47] M. Rakhmanov, Phys. Rev. D **50**, 5155 (1994)
[48] S. Gubser, I. Klebanov, and A. Polyakov, Phys. Lett. B **428**, 105 (1998)
[49] E. Witten, *Anti de sitter space and holography*, (1998), arXiv: hep-th/9802150[hep-th]
[50] J. Maldacena, International Journal of Theoretical Physics **38**, 1113 (1999)
[51] O. Aharony, S. S. Gubser, J. Maldacena *et al.*, Physics Reports **323**, 183 (2000)
[52] D. Klemm and W. Sabra, Phys. Lett. B **503**, 147 (2001)
[53] B. Koch and F. Saueressig, Int. J. Mod. Phys. A **29**, 1430011 (2014)
[54] Á. Rincón, E. Contreras, P. Bargueño *et al.*, Eur. Phys. J. C **77** (2017)
[55] B. Koch and I. Ramirez, Class. Quantum Gravity **28**, 055008 (2011)
[56] B. Koch, I. A. Reyes, and Á. Rincón, Class. Quantum Gravity **33**, 225010 (2016)
[57] A. Bonanno and M. Reuter, Phys. Rev. D **60** (1999)
[58] A. Bonanno, A.-P. Khosravi, and F. Saueressig, Phys. Rev. D **103** (2021)
[59] A. Bonanno and F. Saueressig, *Stability properties of regular black holes*, (2022), arXiv: 2211.09192[gr-qc]
[60] A. Bonanno, A.-P. Khosravi, and F. Saueressig, Phys. Rev. D **107** (2023)
[61] M. A. Abramowicz and P. C. Fragile, Living Rev. Relativ. **16**, 1 (2013), arXiv:1104.5499[astro-ph.HE]
[62] S. Yu, J. Qiu, and C. Gao, Classical and Quantum Gravity **38**, 105006 (2021)
[63] C. J. Gao and S. N. Zhang, Phys. Rev. D **70**, 124019 (2004), arXiv:hep-th/0411104[astro-ph]
[64] I. D. Novikov and K. S. Thorne, in *Black Holes (Les Astres Occlus)* (1973) pp. 343–450.
[65] A. H. Bokhari, J. Rayimbaev, and B. Ahmedov, Phys. Rev. D **102**, 124078 (2020)
[66] J. Rayimbaev, S. Shaymatov, and M. Jamil, Eur. Phys. J. C **81**, 699 (2021), arXiv:2107.13436[gr-qc]
[67] I. D. Novikov and K. S. Thorne, *Astrophysics of black holes* (Gordon and Breach, Science Publishers, Inc, United States, 1973)
[68] D. N. Page and K. S. Thorne, Astrophys. J. **191**, 499 (1974)
[69] B. Narzilloev and B. Ahmedov, Symmetry 14 (2022)
[70] J. M. Bardeen, in *Black Holes (Les Astres Occlus)*, edited by C. Dewitt and B. S. Dewitt (1973) pp. 215–239
[71] C. W. Misner, K. S. Thorne, and J. A. Wheeler, *Gravitation* (W. H. Freeman, San Francisco, 1973)
[72] S. L. Shapiro and S. A. Teukolsky, *Black Holes, White Dwarfs, and Neutron Stars* (John Wiley & Sons, New York, 1983)
[73] S. Shaymatov, P. Sheoran, and S. Siwach, Phys. Rev. D **105**, 104059 (2022), arXiv:2110.10610[gr-qc]
[74] S. Shaymatov, M. Jamil, K. Jusufi *et al.*, Eur. Phys. J. C **82**, 636 (2022), arXiv:2205.00270[gr-qc]
[75] N. Kurbonov, J. Rayimbaev, M. Alloqulov *et al.*, The European Physical Journal C **83**, 506 (2023)
[76] E. Kurmanov, K. Boshkayev, R. Giambò *et al.*, The Astrophysical Journal **925**, 210 (2022)
[77] N. I. Shakura and R. A. Sunyaev, Astron. Astrophys. **24**, 337 (1973)
[78] K. S. Thorne, Astrophys. J. **191**, 507 (1974)
[79] K. Boshkayev, A. Idrissov, O. Luongo *et al.*, Mon. Not. Roy. Astron. Soc. **496**, 1115 (2020), arXiv:2006.01269[astro-ph.HE]
[80] S. Shaymatov, K. Jusufi, M. Alloqulov, *et al.*, Eur. Phys. J. Plus **138**, 997 (2023)